IEEE Access
Multidisciplinary | Rapid Review | Open Access Journal

Received 2 April 2023, accepted 22 April 2023, date of publication 8 May 2023, date of current version 11 May 2023.

Digital Object Identifier 10.1109/ACCESS.2023.3273603

RESEARCH ARTICLE

Data-Driven Model-Free Adaptive Positioning and Anti-Swing Control for Bridge Cranes

XUEJUAN SHAO[1], XIUJIAN ZOU[1], JINGGANG ZHANG[1], ZHICHENG ZHAO[1], ZHIMEI CHEN[1], LIANGLIANG ZHOU[2], AND ZHENYAN WANG[1]

[1]College of Electronic Information Engineering, Taiyuan University of Science and Technology, Taiyuan 030024, China
[2]Taiyuan Heavy Industry Company Ltd., Taiyuan 030024, China

Corresponding authors: Xuejuan Shao (sxj0351@163.com) and Xiujian Zou (2563600856@qq.com)

This work was supported in part by the Shanxi Provincial Key Research and Development Fund under Project 202102020101013, in part by the Doctoral Foundation of the Taiyuan University of Science and Technology under Grant 20202070, and in part by the National Science Foundation of Shanxi Province under Grant 202103021224271.

ABSTRACT In the positioning and anti-swing control of bridge crane, a model-free adaptive control (MFAC) based on data-driven is proposed in order to eliminate the dependence of controller design on the model and the influence of unmodeled dynamics and uncertain disturbances on the controller performance. Only using the input and output data of the bridge crane system, the virtual full format dynamic linearized data model of the bridge crane nonlinear system is obtained through the data-driven modeling method. On the basis of this virtual data model, a model-free adaptive control law and a pseudo-Jacobian matrix estimation algorithm are designed according to the optimization theory under the constraint conditions. The stability of the closed loop system and the convergence of the system error are analyzed and proved by Lipschitz condition and inequality theory. The effectiveness of the control strategy for positioning and anti-swing control of bridge cranes is verified on simulated simulation and experimental platform of bridge crane. The results show that the proposed method is feasible and has good anti-disturbance performance and robustness.

INDEX TERMS Bridge crane, data-driven control, dynamic linearized data model, model-free adaptive control.

I. INTRODUCTION

In the current large-scale production industry, bridge cranes are the most widely used transportation tools and mainly used for loading and transporting goods. However, in the process of work, due to the strong coupling between system states and the influence of uncertain disturbance factors, whether the goods can reach the designated position accurately and quickly during the transportation and whether the load swing angle is within the allowable range are the fundamental problems to be solved [1], [2].

In order to solve the positioning and anti-swing control problems of bridge crane systems, domestic and foreign scholars have made in-depth research. At present, the positioning and anti-swing control methods for bridge cranes are mainly designed based on the system model, such as sliding mode control [3], [4], predictive control [5], [6], active disturbance rejection control [7], [8], robust control [9], [10] and other control methods. In [4], a hierarchical global fast terminal sliding mode control is designed to reduce the disturbance of rope length change and system uncertainty on the control performance, and the simulation results show that the control method can achieve good trolley positioning and load anti-swing control. Reference [6] proposes a novel control approach based on a multivariable model predictive control and a particle swarm optimizer for limiting the transient and residual swing of a payload transferred by an overhead crane and the experimental research proves the effectiveness of the control method. In [8], an active disturbance rejection controller is designed to improve the anti-disturbance and anti-swing performance of the bridge crane. The controller parameters are improved through the salp algorithm. The experimental results show that the controller has significantly improved the anti-disturbance performance of the system.

The associate editor coordinating the review of this manuscript and approving it for publication was Azwirman Gusrialdi.

Reference [10] introduces approximate linearization method and iterative algorithm to establish the linearized equivalent model of the bridge crane system and uses a nonlinear H-infinity control to compensate the modeling error. The results show that the method is robust to modelling errors and external disturbance.

Although the above methods can realize the positioning and anti-swing control of the bridge crane system, they are all model-based control methods. The actual bridge crane system is a very complex nonlinear system, and the precise modeling results of the system cannot be obtained by using mathematical theory or system identification theory. The controller design of data-driven control does not depend on the model of the system itself. The controller design is only conducted through offline or real-time online input and output data of the controlled system. At present, the data-driven control method has been developed and improved continuously, and has been recognized symbolically at home and abroad [11], [12], among which PID control [13], [14], iterative learning control [15], [16], iterative feedback tuning [17], [18], approximate dynamic programming [19], [20] and other methods have been widely used.

Model-free adaptive control is a kind of data-driven control. By introducing the concepts of pseudo partial derivative, pseudo gradient and pseudo-Jacobian matrix, and adopting dynamic linearization technology, the nonlinear relationship of the original system in the whole operation process is equivalent to the system with linear input and output at each working point. Then the controller is designed according to the optimization theory under constraint conditions [21], [22] by minimizing the criterion function of expected output and actual output. At present, mode-free adaptive control strategy has been successfully applied to tower crane system [23], quad rotor unmanned aerial vehicle [24], synchronous motor [25] and other systems, but no scholar has designed model-free adaptive control strategy for bridge crane system.

The bridge crane system is nonlinear, multivariable and strong coupling system, so it is difficult to obtain an accurate mathematical model of the system. In this paper, a filtering error signal is introduced and the full format dynamic linearization method is adopted to establish the dynamic linearization data model of the bridge crane based on input and output data. The controller is designed by using the optimization theory under constraint conditions and the model-free adaptive control theory. The stability of the closed loop system and the boundedness of the system error are proved by Lipschitz condition and inequality theory. Finally, simulation and experimental results demonstrate the feasibility and effectiveness of the proposed method.

The innovation and contribution of this paper are summarized in the following three aspects:

1) A virtual dynamic linearized data model of bridge crane is established by using only the input and output data of the crane system. Therefore, the influence of unmodeled dynamics and system model parameter uncertainties can be avoided.

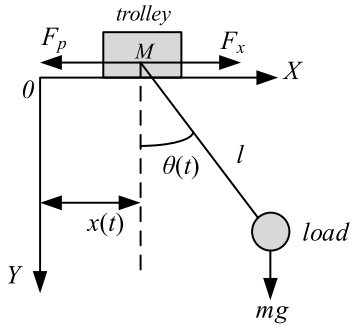

FIGURE 1. 2-D bridge crane system structure diagram.

2) A data-driven model-free adaptive control method is designed based on the virtual dynamic linearized data model for bridge crane, which doesn't require the system dynamic nonlinear model. This method can easily obtain the stability control of the system and is applied to the bridge system for the first time.

3) The algorithm proposed in this paper has strong anti-disturbance ability and has been used for real-time control of bridge cranes on an experimental platform.

The rest of this paper is arranged as follows. In Section II the dynamic model of 2-D bridge crane is introduced and gives the conversion process of bridge crane dynamic linearization data model. In Section III, model-free adaptive control algorithm and Pseudo-Jacobian matrix are designed. Section IV presents the stability analysis of the control system. Section V exhibits the simulation and experimental results, and compares the proposed method with the reference method. In Section VI, the main work of this paper is summarized.

II. SYSTEM MATHEMATICAL MODEL

A. SYSTEM DYNAMICS MODEL

The structure diagram of 2-D bridge crane system is shown in Fig. 1, where l, M and m are the length of rope, the masses of the trolley and load respectively. $x(t)$, $\theta(t)$ is horizontal displacement of the trolley and the swing angle of the load with respect to the vertical respectively. g is the gravitational acceleration. F_x denotes the control input on the trolley. $F_p = p\dot{x}$ represents the rail friction force during trolley movement and p is the friction coefficient between the trolley and the rail.

The dynamic model of 2-D bridge crane system with constant rope length can be described as follows:

$$\boldsymbol{B}(\boldsymbol{q})\ddot{\boldsymbol{q}} + \boldsymbol{C}(\boldsymbol{q}, \dot{\boldsymbol{q}})\dot{\boldsymbol{q}} + \boldsymbol{G}(\boldsymbol{q}) = \boldsymbol{A}u \tag{1}$$

where $\boldsymbol{q} = \begin{bmatrix} x(t) & \theta(t) \end{bmatrix}^T$ denotes the system state vector, $\boldsymbol{B}(\boldsymbol{q})$ is the inertia matrix which is symmetric and positive, $\boldsymbol{C}(\boldsymbol{q}, \dot{\boldsymbol{q}})$ is the centripetal Coriolis matrix, $\boldsymbol{G}(\boldsymbol{q})$ and u represent the gravity vector and the control input respectively. They are

provided as follows:

$$\boldsymbol{B}(\boldsymbol{q}) = \begin{bmatrix} M+m & ml\cos\theta \\ ml\cos\theta & ml^2 \end{bmatrix} \tag{2}$$

$$\boldsymbol{C}(\boldsymbol{q},\dot{\boldsymbol{q}}) = \begin{bmatrix} p & -ml\dot{\theta}\sin\theta \\ 0 & 0 \end{bmatrix} \tag{3}$$

$$\boldsymbol{G}(\boldsymbol{q}) = \begin{bmatrix} 0 & mgl\sin\theta \end{bmatrix}^{\mathrm{T}} \tag{4}$$

$$\boldsymbol{A} = \begin{bmatrix} 1 & 0 \end{bmatrix}^{\mathrm{T}} \tag{5}$$

$$u = F_x \tag{6}$$

B. DYNAMICS LINEARIZATION DATA MODEL

In the control system, the controller is designed to minimize the error between the expected output and the actual output of the system, so the error signal $\boldsymbol{e}(t) \in \mathbb{R}^{2\times 1}$ is defined as

$$\boldsymbol{e}(t) = \boldsymbol{q_d} - \boldsymbol{q} \tag{7}$$

where $\boldsymbol{q_d} = \begin{bmatrix} x_d & \theta_d \end{bmatrix}^T$ is the expected output of the system. x_d denotes the trolley target displacement and θ_d is the desired load swing angle.

In order to facilitate the conversion of bridge crane dynamic linearization data model, the following filtering error signal $\boldsymbol{r}(t) \in \mathbb{R}^{2\times 1}$ of the system is introduced.

$$\boldsymbol{r}(t) = \dot{\boldsymbol{e}} + \boldsymbol{\alpha e} = (\dot{\boldsymbol{q}}_{\boldsymbol{d}} - \dot{\boldsymbol{q}}) + \boldsymbol{\alpha} \times (\boldsymbol{q_d} - \boldsymbol{q}) \tag{8}$$

where $\boldsymbol{\alpha} = \mathrm{diag}\{\alpha_1, \alpha_2\}$ is the positive definite symmetric gain matrix.

The first derivative of signal $\boldsymbol{r}(t)$ with respect to time is

$$\dot{\boldsymbol{r}}(t) = (\ddot{\boldsymbol{q}}_{\boldsymbol{d}} - \ddot{\boldsymbol{q}}) + \boldsymbol{\alpha} \times (\dot{\boldsymbol{q}}_{\boldsymbol{d}} - \dot{\boldsymbol{q}}) \tag{9}$$

There exists $\|\boldsymbol{B}\| \neq 0$. Now multiplying (1) on the left and right by $\boldsymbol{B}^{-1}$, we may rewrite (2) as

$$\ddot{\boldsymbol{q}} + \boldsymbol{B}^{-1}\boldsymbol{C}\dot{\boldsymbol{q}} + \boldsymbol{B}^{-1}\boldsymbol{G} = \boldsymbol{B}^{-1}\boldsymbol{A}u \tag{10}$$

Substitute (10) into (9), and the open-loop dynamic equation based on filtering error signal is

$$\dot{\boldsymbol{r}}(t) = (\boldsymbol{\alpha} - \boldsymbol{B}^{-1}\boldsymbol{C})\boldsymbol{r} + \boldsymbol{B}^{-1}\boldsymbol{C}(\dot{\boldsymbol{q}}_{\boldsymbol{d}} + \boldsymbol{\alpha e}) + \ddot{\boldsymbol{q}}_{\boldsymbol{d}} - \boldsymbol{\alpha}^{\boldsymbol{2}}\boldsymbol{e} + \boldsymbol{B}^{-1}\boldsymbol{G} - \boldsymbol{B}^{-1}\boldsymbol{A}u \tag{11}$$

Define

$$\boldsymbol{N}(\dot{\boldsymbol{q}}_{\boldsymbol{d}}, \ddot{\boldsymbol{q}}_{\boldsymbol{d}}, \boldsymbol{q}, \dot{\boldsymbol{q}}, \ddot{\boldsymbol{q}}) = \boldsymbol{B}^{-1}\boldsymbol{C}(\dot{\boldsymbol{q}}_{\boldsymbol{d}} + \boldsymbol{\alpha e}) + \ddot{\boldsymbol{q}}_{\boldsymbol{d}} + \boldsymbol{B}^{-1}\boldsymbol{G} - \boldsymbol{\alpha}^{\boldsymbol{2}}\boldsymbol{e} \tag{12}$$

Then Eq. (11) can be written as

$$\dot{\boldsymbol{r}}(t) = (\boldsymbol{\alpha} - \boldsymbol{B}^{-1}\boldsymbol{C})\boldsymbol{r} + \boldsymbol{N} - \boldsymbol{B}^{-1}\boldsymbol{A}u \tag{13}$$

Using the forward Euler discretization method, we can have

$$\dot{\boldsymbol{r}}(k) = \frac{\boldsymbol{r}(k+1) - \boldsymbol{r}(k)}{T} \tag{14}$$

where the sampling time T is 0.01s and k is a positive integer greater than zero.

Let $\boldsymbol{y}(k) = \boldsymbol{r}(k)$ and (13) can be converted into the following form:

$$\dot{\boldsymbol{y}}(k) = \frac{\boldsymbol{\alpha B}(k) - \boldsymbol{C}(k)}{\boldsymbol{B}(k)}\boldsymbol{y}(k) - \frac{\boldsymbol{A}u(k)}{\boldsymbol{B}(k)} + \boldsymbol{N}(k) \tag{15}$$

Substituting (14) into (15) has

$$\boldsymbol{y}(k+1) = [\boldsymbol{I} + \frac{\boldsymbol{\alpha B}(k) - \boldsymbol{C}(k)}{\boldsymbol{B}(k)} \times T]\boldsymbol{y}(k) - \frac{\boldsymbol{A}u(k)}{\boldsymbol{B}(k)} \times T + \boldsymbol{N}(k) \times T \tag{16}$$

Therefore, the relationship between the input and output of the bridge crane system has been obtained. (16) provides the basis for whether the subsequent bridge crane system can be converted into a linear model with standard input and output changes, and whether the model-free adaptive control method can be used. So, the following assumptions are made to analyze (16).

Assumption 1: The partial derivative of $\boldsymbol{y}(k+1)$ with respect to $\boldsymbol{y}(k)$ and $u(k)$ are continuous.

Assumption 2: (16) satisfies the generalized Lipschitz condition, that is, for any $k_1 \geq 0, k_2 \geq 0, b' > 0$ and $k_1 \neq k_2$, $\boldsymbol{H}(k_1) \neq \boldsymbol{H}(k_2)$, the following inequality holds.

$$\|\boldsymbol{y}(k_1+1) - \boldsymbol{y}(k_2+1)\| \leq b' \|\boldsymbol{H}(k_1) - \boldsymbol{H}(k_2)\| \tag{17}$$

where $\boldsymbol{H}(k) = \begin{bmatrix} \boldsymbol{y}(k) & u(k) \end{bmatrix}^{\mathrm{T}}$.

According to the definition of partial derivative there are the following formulas.

$$\begin{aligned} &\lim_{\Delta \boldsymbol{y}(k)\to 0} \frac{f(\boldsymbol{y}(k) + \Delta \boldsymbol{y}(k)) - f(\boldsymbol{y}(k))}{\Delta \boldsymbol{y}(k)} \\ &= \lim_{\Delta \boldsymbol{y}(k)\to 0} \frac{[\boldsymbol{I} + \frac{\boldsymbol{\alpha B}(k) - \boldsymbol{C}(k)}{\boldsymbol{B}(k)} \times T] \times \Delta \boldsymbol{y}(k)}{\Delta \boldsymbol{y}(k)} \\ &= \boldsymbol{I} + \frac{\boldsymbol{\alpha B}(k) - \boldsymbol{C}(k)}{\boldsymbol{B}(k)} \times T \end{aligned} \tag{18}$$

$$\begin{aligned} &\lim_{\Delta u(k)\to 0} \frac{f(u(k) + \Delta u(k)) - f(u(k))}{\Delta u(k)} \\ &= \lim_{\Delta u(k)\to 0} \frac{-\frac{\boldsymbol{A}}{\boldsymbol{B}(k)} \times T \times \Delta u(k)}{\Delta u(k)} \\ &= -\frac{\boldsymbol{A}}{\boldsymbol{B}(k)} \times T \end{aligned} \tag{19}$$

Continuous partial derivative of $\boldsymbol{y}(k+1)$ for $\boldsymbol{y}(k)$ and $u(k)$ exists. Therefore, (16) satisfies Assumption 1.

In (2) and (3), $\theta(k)$ changes very little at adjacent moments, so it can be ignored. Let $\boldsymbol{B}(k_1) = \boldsymbol{B}(k_2), \boldsymbol{C}(k_1) = \boldsymbol{C}(k_2)$, there is

$$\begin{aligned} &\boldsymbol{y}(k_1+1) - \boldsymbol{y}(k_2+1) \\ &= [\boldsymbol{I} + \frac{\boldsymbol{\alpha B}(k_1) - \boldsymbol{C}(k_1)}{\boldsymbol{B}(k_1)} \times T] \times [\boldsymbol{y}(k_1) - \boldsymbol{y}(k_2)] \\ &\quad - \frac{\boldsymbol{A}T}{\boldsymbol{B}(k_1)}[u(k_1) - u(k_2)] + T[\boldsymbol{N}(k_1) - \boldsymbol{N}(k_2)] \\ &= \begin{bmatrix} I + \frac{\boldsymbol{\alpha B}(k_1) - \boldsymbol{C}(k_1)}{\boldsymbol{B}(k_1)} \times T & -\frac{\boldsymbol{A}T}{\boldsymbol{B}(k_1)} \end{bmatrix} \end{aligned}$$

$$\times \begin{bmatrix} \boldsymbol{y}(k_1)-\boldsymbol{y}(k_2) \\ u(k_1)-u(k_2) \end{bmatrix} + T[\boldsymbol{N}(k_1)-\boldsymbol{N}(k_2)] \tag{20}$$

Because $\|\boldsymbol{H}(k_1)-\boldsymbol{H}(k_2)\| = \left\| \begin{bmatrix} \boldsymbol{y}(k_1)-\boldsymbol{y}(k_2) \\ u(k_1)-u(k_2) \end{bmatrix} \right\| \neq 0$, there is

$$\begin{aligned} &\frac{\|\boldsymbol{y}(k_1+1)-\boldsymbol{y}(k_2+1)\|}{\left\| \begin{bmatrix} \boldsymbol{y}(k_1)-\boldsymbol{y}(k_2) \\ u(k_1)-u(k_2) \end{bmatrix} \right\|} \\ &\leq \left\| \begin{bmatrix} \boldsymbol{I}+\dfrac{\boldsymbol{\alpha B}(k_1)-\boldsymbol{C}(k_1)}{\boldsymbol{B}(k_1)}\times T & -\dfrac{\boldsymbol{AT}}{\boldsymbol{B}(k_1)} \end{bmatrix} \right\| \\ &\quad + \frac{\|T[\boldsymbol{N}(k_1)-\boldsymbol{N}(k_2)]\|}{\left\| \begin{bmatrix} \boldsymbol{y}(k_1)-\boldsymbol{y}(k_2) \\ u(k_1)-u(k_2) \end{bmatrix} \right\|} \end{aligned} \tag{21}$$

Because $\left\| \boldsymbol{I}+\frac{\boldsymbol{\alpha B}(k_1)-\boldsymbol{C}(k_1)}{\boldsymbol{B}(k_1)}\times T \quad -\frac{\boldsymbol{AT}}{\boldsymbol{B}(k_1)} \right\|$ and $\|\boldsymbol{N}(k_1)-\boldsymbol{N}(k_2)\|$ exist at any moment k, therefore, (16) satisfies Assumption 2.

Theorem 1: The bridge crane system is a single-input double-output system. If Assumption 1 and Assumption 2 are satisfied, (16) can be converted into the following bridge crane dynamic linearized data model.

$$\Delta\boldsymbol{y}(k+1) = \boldsymbol{\Phi}(k)\Delta\boldsymbol{H}(k) = \boldsymbol{\phi}_1\Delta\boldsymbol{y}(k) + \boldsymbol{\phi}_2\Delta u(k) \tag{22}$$

in which $\boldsymbol{\Phi}(k) = \begin{bmatrix} \boldsymbol{\phi}_1(k) & \boldsymbol{\phi}_2(k) \end{bmatrix}$ is time-varying Pseudo-Jacobian parameter matrix, $\boldsymbol{\phi}_1(k) \in \mathbb{R}^{2\times 2}$, $0 < \left\|\boldsymbol{\phi}_1(k)\right\| \leq b_1$, $\boldsymbol{\phi}_2(k) \in \mathbb{R}^{2\times 1}$, $0 < \left\|\boldsymbol{\phi}_2(k)\right\| \leq b_2$, $0 < \|\boldsymbol{\phi}(k)\| \leq \sqrt{b_1^2+b_2^2} = b$, $\Delta\boldsymbol{H}(k) = \begin{bmatrix} \Delta\boldsymbol{y}(k) & \Delta u(k) \end{bmatrix}^{\mathrm{T}}$, and b_1, b_2 are all bounded positive numbers.

Proof: According to (16), there is

$$\begin{aligned} &\Delta\boldsymbol{y}(k+1) \\ &= \boldsymbol{y}(k+1)-\boldsymbol{y}(k) \\ &= [\boldsymbol{I}+\frac{\boldsymbol{\alpha B}(k)-\boldsymbol{C}(k)}{\boldsymbol{B}(k)}\times T]\boldsymbol{y}(k) - \frac{\boldsymbol{A}u(k)}{\boldsymbol{B}(k)}\times T \\ &\quad + \boldsymbol{N}(k)\times T - [\boldsymbol{I}+\frac{\boldsymbol{\alpha B}(k-1)-\boldsymbol{C}(k-1)}{\boldsymbol{B}(k-1)}\times T]\boldsymbol{y}(k-1) \\ &\quad + \frac{\boldsymbol{A}u(k-1)}{\boldsymbol{B}(k-1)}\times T - \boldsymbol{N}(k-1)\times T \\ &= [\boldsymbol{I}+\frac{\boldsymbol{\alpha B}(k)-\boldsymbol{C}(k)}{\boldsymbol{B}(k)}\times T]\boldsymbol{y}(k) - \frac{\boldsymbol{A}u(k)}{\boldsymbol{B}(k)}\times T \\ &\quad + \boldsymbol{N}(k)\times T + [\boldsymbol{I}+\frac{\boldsymbol{\alpha B}(k)-\boldsymbol{C}(k)}{\boldsymbol{B}(k)}\times T]\boldsymbol{y}(k-1) \\ &\quad - \frac{\boldsymbol{A}u(k-1)}{\boldsymbol{B}(k)}\times T + \boldsymbol{N}(k)\times T - [\boldsymbol{I}+\frac{\boldsymbol{\alpha B}(k)-\boldsymbol{C}(k)}{\boldsymbol{B}(k)} \\ &\quad \times T]\boldsymbol{y}(k-1) + \frac{\boldsymbol{A}u(k-1)}{\boldsymbol{B}(k)}\times T - \boldsymbol{N}(k)\times T \\ &\quad - [\boldsymbol{I}+\frac{\boldsymbol{\alpha B}(k-1)-\boldsymbol{C}(k-1)}{\boldsymbol{B}(k-1)}\times T]\boldsymbol{y}(k-1) \\ &\quad + \frac{\boldsymbol{A}u(k-1)}{\boldsymbol{B}(k-1)}\times T - \boldsymbol{N}(k-1)\times T \end{aligned} \tag{23}$$

For the convenience of controller design, let

$$\begin{aligned} \boldsymbol{Z}(k) &= [\boldsymbol{I}+\frac{\boldsymbol{\alpha B}(k)-\boldsymbol{C}(k)}{\boldsymbol{B}(k)}T]\boldsymbol{y}(k-1) - \frac{\boldsymbol{A}u(k-1)}{\boldsymbol{B}(k)}T \\ &\quad + \boldsymbol{N}(k)T - [\boldsymbol{I}+\frac{\boldsymbol{\alpha B}(k-1)-\boldsymbol{C}(k-1)}{\boldsymbol{B}(k-1)}T]\boldsymbol{y}(k-1) \\ &\quad + \frac{\boldsymbol{A}u(k-1)}{\boldsymbol{B}(k-1)}\times T - \boldsymbol{N}(k-1)\times T \end{aligned} \tag{24}$$

where $\boldsymbol{Z}(k) \in \mathbb{R}^{2\times 1}$.

According to the definition of partial derivative, the following equations can be obtained.

$$\frac{\partial\boldsymbol{y}(k+1)}{\partial\boldsymbol{y}(k)} = \boldsymbol{I}+\frac{\boldsymbol{\alpha B}(k)-\boldsymbol{C}(k)}{\boldsymbol{B}(k)}\times T \tag{25}$$

$$\frac{\partial\boldsymbol{y}(k+1)}{\partial u(k)} = -\frac{\boldsymbol{A}}{\boldsymbol{B}(k)}\times T \tag{26}$$

Then, (23) can be converted into the following form:

$$\begin{aligned} &\Delta\boldsymbol{y}(k+1) \\ &= [\boldsymbol{I}+\frac{\boldsymbol{\alpha B}(k)-\boldsymbol{C}(k)}{\boldsymbol{B}(k)}T]\boldsymbol{y}(k) - \frac{\boldsymbol{A}u(k)}{\boldsymbol{B}(k)}T + \boldsymbol{N}(k)T \\ &\quad - [\boldsymbol{I}+\frac{\boldsymbol{\alpha B}(k)-\boldsymbol{C}(k)}{\boldsymbol{B}(k)}T]\boldsymbol{y}(k-1) + \frac{\boldsymbol{A}u(k-1)}{\boldsymbol{B}(k)}\times T \\ &\quad - \boldsymbol{N}(k)\times T + \boldsymbol{Z}(k) \\ &= [\boldsymbol{I}+\frac{\boldsymbol{\alpha B}(k)-\boldsymbol{C}(k)}{\boldsymbol{B}(k)}T][\boldsymbol{y}(k)-\boldsymbol{y}(k-1)] - \frac{T}{\boldsymbol{B}(k)} \\ &\quad \times [\boldsymbol{A}u(k)-\boldsymbol{A}u(k-1)] + \boldsymbol{Z}(k) \\ &= \frac{\partial\boldsymbol{y}(k+1)}{\partial\boldsymbol{y}(k)}\times\Delta\boldsymbol{y}(k) + \frac{\partial\boldsymbol{y}(k+1)}{\partial u(k)}\times\Delta u(k) + \boldsymbol{Z}(k) \end{aligned} \tag{27}$$

For a fixed moment k, $\boldsymbol{Z}(k)$ can be expressed as

$$\boldsymbol{Z}(k) = z(k)\times\Delta\boldsymbol{H}(k) \tag{28}$$

where $z(k) \in \mathbb{R}^{2\times 3}$.

For any moment k, $\|\Delta\boldsymbol{H}(k)\| \neq 0$, (28) has at least one non-zero solution $z^*(k)$, so that

$$\boldsymbol{Z}(k) = z^*(k)\times\Delta\boldsymbol{H}(k) \tag{29}$$

Let $\boldsymbol{\Phi}(k) = z^*(k) + \begin{bmatrix} \frac{\partial\boldsymbol{y}(k+1)}{\partial\boldsymbol{y}(k)} & \frac{\partial\boldsymbol{y}(k+1)}{\partial u(k)} \end{bmatrix}$, (27) can be converted to the following form:

$$\Delta\boldsymbol{y}(k+1) = \boldsymbol{\phi}_1(k)\Delta\boldsymbol{y}(k) + \boldsymbol{\phi}_2(k)\Delta u(k) \tag{30}$$

Therefore, the full format dynamic linearized data model of bridge crane system is

$$\begin{aligned} \boldsymbol{y}(k+1) &= \boldsymbol{y}(k) + \boldsymbol{\Phi}(k)\Delta\boldsymbol{H}(k) \\ &= \boldsymbol{y}(k) + \boldsymbol{\phi}_1(k)\Delta\boldsymbol{y}(k) + \boldsymbol{\phi}_2(k)\Delta u(k) \end{aligned} \tag{31}$$

Equation (31) does not contain the information of the system model of the bridge crane and it is only a virtual model which provides the basis for subsequent controller design and system stability analysis.

III. CONTROLLER DESIGN

A. MODEL-FREE ADAPTIVE CONTROL LAW DESIGN

In order to eliminate system deviation, it can be seen from (31) that the input change at the current k moment will affect the output change at the next moment. According to the

optimization theory, the criterion function under constraint conditions can be obtained.

$$J(u(k)) = \left\|\boldsymbol{y_d}(k+1) - \boldsymbol{y}(k+1)\right\|^2 + \lambda \left\|u(k) - u(k-1)\right\|^2 \tag{32}$$

where $\boldsymbol{y_d}(k+1)$ is the filter desired output of the system at the moment $k+1$ and $\lambda > 0$ is the penalty factor for the control input which affects the error of the system.

Substituting (31) into (32) has

$$J(u(k)) = \left\|\boldsymbol{y_d}(k+1) - \boldsymbol{\phi}_1(k)\Delta\boldsymbol{y}(k) - \boldsymbol{\phi}_2(k)\Delta u(k) - \boldsymbol{y}(k)\right\|^2 + \lambda \left\|u(k) - u(k-1)\right\|^2 \tag{33}$$

Then, by differentiating $J(u(k))$ with respect to $u(k)$ and making the result zero, the following equation can be obtained.

$$\left\|-\boldsymbol{\phi}_2(k)\right\| \times \left\|\boldsymbol{y_d}(k+1) - \boldsymbol{\phi}_1(k)\Delta\boldsymbol{y}(k) - \boldsymbol{\phi}_2(k)\Delta u(k) - \boldsymbol{y}(k)\right\| + \lambda(u(k) - u(k-1)) = 0 \tag{34}$$

Thus, the model-free adaptive control law of the bridge crane system is determined as follows:

$$u(k) = u(k-1) + \rho_1 \times \boldsymbol{\phi}_2^{\mathrm{T}}(k) \times \frac{\boldsymbol{y_d}(k+1) - \boldsymbol{y}(k)}{\lambda + \left\|\boldsymbol{\phi}_2(k)\right\|^2} - \rho_2 \times \boldsymbol{\phi}_2^{\mathrm{T}}(k) \times \frac{\boldsymbol{\phi}_1(k)\Delta\boldsymbol{y}(k)}{\lambda + \left\|\boldsymbol{\phi}_2(k)\right\|^2} \tag{35}$$

where $\rho_1 = \rho_2 \in (0, 1]$ are the step size factors to make the algorithm more flexible and general, $\boldsymbol{\phi}_1(k)$ and $\boldsymbol{\phi}_2(k)$ are time-varying parameter matrices which can be obtained by estimation algorithm.

B. THE DESIGN OF PSEUDO-JACOBI MATRIX ESTIMATION ALGORITHM

In order to realize (35), it is necessary to know the exact value of the Pseudo-Jacobian matrix. The model of the bridge crane system is unknown and the Pseudo-Jacobian matrix value is difficult to obtain. Therefore, the estimation algorithm using the system input and output data is adopted.

The traditional parameter estimation criterion function is to minimize the square of the difference between the system model output and the actual output. The model-free adaptive control algorithm can achieve stable control of the system only by using the input and output data of the system. This algorithm requires high data accuracy. In addition, its parameter estimation is too sensitive to data changes caused by disturbance and other factors. So, the following criteria function is used to calculate the time-varying parameters of the Pseudo-Jacobian matrix.

$$J(\boldsymbol{\Phi}(k)) = \left\|\boldsymbol{y}(k) - \boldsymbol{y}(k-1) - \boldsymbol{\Phi}(k)\Delta\boldsymbol{H}(k-1)\right\|^2 + \mu \left\|\boldsymbol{\Phi}(k) - \hat{\boldsymbol{\Phi}}(k-1)\right\|^2 \tag{36}$$

where $\hat{\boldsymbol{\Phi}}(k) = \hat{\boldsymbol{\Phi}}(k-1) + \Delta\boldsymbol{\Phi}(k)$ is the estimated value of $\boldsymbol{\Phi}(k)$, and $\mu > 0$ is the weight factor used to limit the variation of parameter estimation.

For (36), by differentiating $J(\boldsymbol{\Phi}(k))$ with $\boldsymbol{\Phi}(k)$ respect to and making the result zero, we can obtain.

$$\left\|\left(\Delta\boldsymbol{y}(k) - \boldsymbol{\Phi}(k)\Delta\boldsymbol{H}(k-1)\right)\right\| \times \left\|-\Delta\boldsymbol{H}(k-1)\right\| + \mu \left\|\boldsymbol{\Phi}(k) - \hat{\boldsymbol{\Phi}}(k-1)\right\| = 0 \tag{37}$$

The Pseudo-Jacobi matrix estimation algorithm for the model-free adaptive control law of the bridge crane system can be obtained by simplifying (37) as follows.

$$\hat{\boldsymbol{\Phi}}(k) = \hat{\boldsymbol{\Phi}}(k-1) + \eta \times \frac{1}{\mu + \left\|\Delta\boldsymbol{H}(k-1)\right\|^2} \times \left(\Delta\boldsymbol{y}(k) - \hat{\boldsymbol{\Phi}}(k-1) \times \Delta\boldsymbol{H}(k-1)\right) \times \left(\Delta\boldsymbol{H}(k-1)\right)^{\mathrm{T}} \tag{38}$$

where $\eta \in (0, 2]$ is the step size factor which makes the algorithm more flexible and general.

$$\hat{\boldsymbol{\phi}}_1(k) = \hat{\boldsymbol{\phi}}_1(k-1) + \eta \times \frac{1}{\mu + \left\|\Delta\boldsymbol{H}(k-1)\right\|^2} \times \left(\Delta\boldsymbol{y}(k) - \hat{\boldsymbol{\Phi}}(k-1) \times \Delta\boldsymbol{H}(k-1)\right) \times \left(\Delta\boldsymbol{y}(k-1)\right)^{\mathrm{T}} \tag{39}$$

$$\hat{\boldsymbol{\phi}}_2(k) = \hat{\boldsymbol{\phi}}_2(k-1) + \eta \times \frac{1}{\mu + \left\|\Delta\boldsymbol{H}(k-1)\right\|^2} \times \left(\Delta\boldsymbol{y}(k) - \hat{\boldsymbol{\Phi}}(k-1) \times \Delta\boldsymbol{H}(k-1)\right) \times \left(\Delta u(k-1)\right) \tag{40}$$

where $\hat{\boldsymbol{\phi}}_1(k)$ and $\hat{\boldsymbol{\phi}}_2(k)$ are the estimated values of $\boldsymbol{\phi}_1(k)$ and $\boldsymbol{\phi}_2(k)$, respectively. $\boldsymbol{\phi}_1(k)$ represents the linear relationship of filtering error output at any moment k and $\boldsymbol{\phi}_2(k)$ represents the linear relationship of filtering error output and input at any moment k.

Since $\hat{\boldsymbol{\phi}}_1(k)$ and $\hat{\boldsymbol{\phi}}_2(k)$ are real-time changing values, the following reset algorithm is introduced to reduce the impact on control performance caused by excessive or small estimation tracking error.

If $\left\|\hat{\boldsymbol{\phi}}_i(k)\right\| \leq c$ or $\left\|\hat{\boldsymbol{\phi}}_i(k)\right\| > ac$ or $\mathrm{sign}(\hat{\boldsymbol{\phi}}_i(k)) \neq \mathrm{sign}(\hat{\boldsymbol{\phi}}_i(1))$, then $\hat{\boldsymbol{\phi}}_i(k) \neq \hat{\boldsymbol{\phi}}_i(1)$ $(i = 1, 2)$, where $\hat{\boldsymbol{\phi}}_i(1)$ is the initial value of $\hat{\boldsymbol{\phi}}_i(k)$, a is a very large positive number and c is a very small positive number.

In summary, the proposed control method can be summarized as the following steps.

(1) Set the initial parameters λ, ρ_1, ρ_2, μ, η and $\boldsymbol{\phi}_1(1)$, $\boldsymbol{\phi}_2(1)$ of the controller.

(2) Assume the system outputs $\boldsymbol{y}(1) = \boldsymbol{y}(2) = \begin{bmatrix} 0 & 0 \end{bmatrix}^{\mathrm{T}}$ and inputs $u(1) = u(2) = 0$.

(3) Calculate the values of parameters $\hat{\boldsymbol{\phi}}_1(k)$ and $\hat{\boldsymbol{\phi}}_2(k)$ by using the Jacobian estimation algorithm of (39) and (40).

(4) The model-free adaptive control law $u(k)$ is obtained by (35).

IV. STABILITY ANALYSIS

Theorem 2: For the system (16) that satisfies Assumptions 1 and 2, the model-free adaptive control law of (35) and (38) are adopted. When the expected output of the filtering error is constant, that is, $\boldsymbol{y_d}(k+1) = \boldsymbol{y_d}(k) = \mathrm{const}$,

there is a positive number $0 < \lambda_{\min} \leq \lambda$ that makes the system tracking error gradually approach zero, that is, $\lim_{k\to\infty} \|\boldsymbol{y_d}(k+1) - \boldsymbol{y}(k)\| = 0$. And the system is BIBO stable, that is, the output $\boldsymbol{y}(k)$ and input $u(k)$ are bounded.

Proof: **Step 1:** According to the definition, the estimated value of Pseudo-Jacobian matrix changes at different times, so the estimated error of Pseudo-Jacobian matrix is as follows:

$$\tilde{\boldsymbol{\Phi}}(k) = \hat{\boldsymbol{\Phi}}(k) - \boldsymbol{\Phi}(k) \tag{41}$$

Subtract $\boldsymbol{\Phi}(k)$ both sides of (38) at the same time, and (38) is converted into the following form.

$$\begin{aligned}\tilde{\boldsymbol{\Phi}}(k) = {} & \hat{\boldsymbol{\Phi}}(k-1) - \boldsymbol{\Phi}(k-1) + \boldsymbol{\Phi}(k-1) - \boldsymbol{\Phi}(k) \\ & + \eta \times \frac{(\Delta \boldsymbol{y}(k) - \hat{\boldsymbol{\Phi}}(k-1) \times \Delta \boldsymbol{H}(k-1))}{\mu + \|\Delta \boldsymbol{H}(k-1)\|^2} \\ & \times (\Delta \boldsymbol{H}(k-1))^{\mathrm{T}}\end{aligned} \tag{42}$$

The size of the matrix is expressed by two norms, in order to facilitate size comparison the norms on both sides of (42) are taken.

$$\begin{aligned}\left\|\tilde{\boldsymbol{\Phi}}(k)\right\| = {} & \left\|\hat{\boldsymbol{\Phi}}(k-1) - \boldsymbol{\Phi}(k-1) + \boldsymbol{\Phi}(k-1) - \boldsymbol{\Phi}(k)\right. \\ & + \eta \times \frac{\Delta \boldsymbol{y}(k) - \hat{\boldsymbol{\Phi}}(k-1) \times \Delta \boldsymbol{H}(k-1)}{\mu + \|\Delta \boldsymbol{H}(k-1)\|^2} \\ & \left. \times (\Delta \boldsymbol{H}(k-1))^{\mathrm{T}}\right\|\end{aligned} \tag{43}$$

When d_1 and d_2 are arbitrary real numbers, there is $\|d_1 \pm d_2\| \leq \|d_1\| + \|d_2\|$. So (43) can be written in the form of following inequality.

$$\begin{aligned}\left\|\tilde{\boldsymbol{\Phi}}(k)\right\| \leq {} & \left\|\tilde{\boldsymbol{\Phi}}(k-1)\right\| + \|\boldsymbol{\Phi}(k-1)\| + \|\boldsymbol{\Phi}(k)\| \\ & + \left\|\eta \frac{(\Delta \boldsymbol{y}(k) - \hat{\boldsymbol{\Phi}}(k-1) \times \Delta \boldsymbol{H}(k-1))}{\mu + \|\Delta \boldsymbol{H}(k-1)\|^2}\right\| \\ & \times \left\|(\Delta \boldsymbol{H}(k-1))^{\mathrm{T}}\right\|\end{aligned} \tag{44}$$

Since the dynamic linearized data model (31) of the bridge crane system satisfies the generalized Lipschitz condition, that is, $0 < \|\boldsymbol{\phi}(k)\| \leq \sqrt{b_1^2 + b_2^2} = b$, so the following inequality can be combined.

$$\begin{aligned}\tilde{\boldsymbol{\Phi}}(k) \leq {} & \left\|\tilde{\boldsymbol{\Phi}}(k-1)\right\| + b + b \\ & + \left\|\eta \frac{(\Delta \boldsymbol{y}(k) - \hat{\boldsymbol{\Phi}}(k-1) \times \Delta \boldsymbol{H}(k-1))}{\mu + \|\Delta \boldsymbol{H}(k-1)\|^2}\right\| \\ & \times \left\|(\Delta \boldsymbol{H}(k-1))^{\mathrm{T}}\right\|\end{aligned} \tag{45}$$

in which there is

$$\begin{aligned}& \left\|\eta \frac{(\Delta \boldsymbol{y}(k) - \hat{\boldsymbol{\Phi}}(k-1) \times \Delta \boldsymbol{H}(k-1))}{\mu + \|\Delta \boldsymbol{H}(k-1)\|^2}\right\| \times \left\|(\Delta \boldsymbol{H}(k-1))^{\mathrm{T}}\right\| \\ & \leq \eta \times \left\|\frac{\Delta \boldsymbol{y}(k)}{\mu + \|\Delta \boldsymbol{H}(k-1)\|^2} \times (\Delta \boldsymbol{H}(k-1))^{\mathrm{T}}\right\| \\ & + \eta \times \left\|\frac{\hat{\boldsymbol{\Phi}}(k-1) \times \Delta \boldsymbol{H}(k-1)}{\mu + \|\Delta \boldsymbol{H}(k-1)\|^2} \times (\Delta \boldsymbol{H}(k-1))^{\mathrm{T}}\right\|\end{aligned} \tag{46}$$

Due to $\left\|\Delta \boldsymbol{H}(k-1) \times (\Delta \boldsymbol{H}(k-1))^{\mathrm{T}}\right\| = \|\Delta \boldsymbol{H}(k-1)\|^2$ and $\|d_1 + d_2\| \geq 2\sqrt{d_1 d_2}$, let $\|\Delta y(k)\| \leq \varepsilon_1$ and $\|\Delta H(k-1)\| \leq \varepsilon_2$, where ε_1 and ε_2 are any small positive numbers, there is

$$\begin{aligned}& \eta \times \left\|\frac{\Delta \boldsymbol{y}(k)}{\mu + \|\Delta \boldsymbol{H}(k-1)\|^2} \times (\Delta \boldsymbol{H}(k-1))^{\mathrm{T}}\right\| \\ & = \eta \times \left\|\frac{\Delta \boldsymbol{y}(k)}{\frac{\mu}{\|\Delta \boldsymbol{H}(k-1)\|} + \|\Delta \boldsymbol{H}(k-1)\|}\right\| \\ & \leq \eta \times \frac{\varepsilon_1}{2\sqrt{\mu}}\end{aligned} \tag{47}$$

$$\begin{aligned}& \eta \times \left\|\frac{\hat{\boldsymbol{\Phi}}(k-1) \times \Delta \boldsymbol{H}(k-1)}{\mu + \|\Delta \boldsymbol{H}(k-1)\|^2} \times (\Delta \boldsymbol{H}(k-1))^{\mathrm{T}}\right\| \\ & = \eta \times \left\|\tilde{\boldsymbol{\Phi}}(k-1) + \boldsymbol{\Phi}(k-1)\right\| \times \left\|\frac{\|\Delta \boldsymbol{H}(k-1)\|^2}{\mu + \|\Delta \boldsymbol{H}(k-1)\|^2}\right\| \\ & = \eta \times \left\|\tilde{\boldsymbol{\Phi}}(k-1) + \boldsymbol{\Phi}(k-1)\right\| \times \frac{1}{\frac{\mu}{\|\Delta \boldsymbol{H}(k-1)\|^2} + 1} \\ & \leq \eta \times \left\|\tilde{\boldsymbol{\Phi}}(k-1) + \boldsymbol{\Phi}(k-1)\right\| \times \frac{\|\Delta \boldsymbol{H}(k-1)\|}{2\sqrt{\mu}} \\ & \leq \eta \times \left\|\tilde{\boldsymbol{\Phi}}(k-1)\right\| \times \frac{\varepsilon_2}{2\sqrt{\mu}} + \eta \times b \frac{\varepsilon_2}{2\sqrt{\mu}}\end{aligned} \tag{48}$$

In the end, there is

$$\begin{aligned}\left\|\tilde{\boldsymbol{\Phi}}(k)\right\| \leq {} & \left\|\tilde{\boldsymbol{\Phi}}(k-1)\right\| + b + b + \eta \frac{\varepsilon_1}{2\sqrt{\mu}} \\ & + \eta \left\|\tilde{\boldsymbol{\Phi}}(k-1)\right\| \frac{\varepsilon_2}{2\sqrt{\mu}} + \eta b \frac{\varepsilon_2}{2\sqrt{\mu}}\end{aligned} \tag{49}$$

By sorting out the above inequalities, we can obtain

$$\left\|\tilde{\boldsymbol{\Phi}}(k)\right\| \leq \frac{2\sqrt{\mu} + \eta\varepsilon_2}{2\sqrt{\mu}} \left\|\tilde{\boldsymbol{\Phi}}(k-1)\right\| + 2b + \frac{\eta\varepsilon_1 + \eta b\varepsilon_2}{2\sqrt{\mu}} \tag{50}$$

Let $\varepsilon = 2b + \frac{\eta\varepsilon_1 + \eta b\varepsilon_2}{2\sqrt{\mu}} = \frac{4b\sqrt{\mu} + \eta\varepsilon_1 + \eta b\varepsilon_2}{2\sqrt{\mu}}$ and $\tau = 1 + \frac{\eta\varepsilon_2}{2\sqrt{\mu}} = \frac{2\sqrt{\mu} + \eta\varepsilon_2}{2\sqrt{\mu}}$, through recursive reasoning there is

$$\begin{aligned}\left\|\tilde{\boldsymbol{\Phi}}(k)\right\| & \leq \tau \left\|\tilde{\boldsymbol{\Phi}}(k-1)\right\| + \varepsilon \\ & \leq \tau \times \tau \times \left\|\tilde{\boldsymbol{\Phi}}(k-2)\right\| + \tau\varepsilon + \varepsilon \\ & \leq \tau^{k-1} \left\|\tilde{\boldsymbol{\Phi}}(1)\right\| + \frac{\varepsilon(1-\tau^{k-1})}{1-\tau}\end{aligned} \tag{51}$$

where

$$\tau^{k-1} = \left(\frac{2\sqrt{\mu} + \eta\varepsilon_2}{2\sqrt{\mu}}\right)^{k-1} = \left(1 + \frac{\eta\varepsilon_2}{2\sqrt{\mu}}\right)^{k-1} \tag{52}$$

$$\frac{\varepsilon(1-\tau^{k-1})}{1-\tau} = \frac{4b\sqrt{\mu} + \eta\varepsilon_1 + \eta b\varepsilon_2}{2\sqrt{\mu}} \times \frac{1 - \left(\frac{2\sqrt{\mu} + \eta\varepsilon_2}{2\sqrt{\mu}}\right)^{k-1}}{-\frac{\eta\varepsilon_2}{2\sqrt{\mu}}}$$

$$= \frac{4b\sqrt{\mu}+\eta\varepsilon_1+\eta b\varepsilon_2}{-\eta\varepsilon_2} \times (1-(\frac{2\sqrt{\mu}+\eta\varepsilon_2}{2\sqrt{\mu}})^{k-1}) \tag{53}$$

In (52) and (53), μ, η, b, ε_1, ε_2 are bounded values and $\tilde{\boldsymbol{\Phi}}(1) = \hat{\boldsymbol{\Phi}}(1) - \boldsymbol{\Phi}(1)$, $\boldsymbol{\Phi}(1)$ is an initial value. Therefore, $\tilde{\boldsymbol{\Phi}}(k) = \hat{\boldsymbol{\Phi}}(k) - \boldsymbol{\Phi}(k)$ is bounded. And $0 < \|\boldsymbol{\phi}(k)\| \leq b$, so $\hat{\boldsymbol{\Phi}}(k)$ is also bounded.

Step 2: The system tracking error is defined as follows.

$$\boldsymbol{E}(k+1) = \boldsymbol{y_d}(k+1) - \boldsymbol{y}(k+1) \tag{54}$$

Substitute (31) into (54) and $\boldsymbol{y}_d(k+1) = \boldsymbol{y}_d(k) = \text{const}$, so there is

$$\begin{aligned}
&\boldsymbol{E}(k+1)\\
&= \boldsymbol{y_d}(k+1) - \boldsymbol{y}(k+1)\\
&= \boldsymbol{y_d}(k+1) - \boldsymbol{y}(k) - \boldsymbol{\phi}_1(k)\Delta\boldsymbol{y}(k) - \boldsymbol{\phi}_2(k)\Delta u(k)\\
&= \boldsymbol{E}(k) - \boldsymbol{\phi}_1(k)\Delta\boldsymbol{y}(k) - \boldsymbol{\phi}_2(k) \times (\rho_1 \times \boldsymbol{\phi}_2^{\mathrm{T}}(k)\\
&\quad \times \frac{\boldsymbol{y_d}(k+1) - \boldsymbol{y}(k)}{\lambda + \left\|\boldsymbol{\phi}_2(k)\right\|^2} - \rho_2 \times \boldsymbol{\phi}_2^{\mathrm{T}}(k) \times \frac{\boldsymbol{\phi}_1(k)\Delta\boldsymbol{y}(k)}{\lambda + \left\|\boldsymbol{\phi}_2(k)\right\|^2})\\
&= [I - \frac{\rho_1\boldsymbol{\phi}_2(k) \times \boldsymbol{\phi}_2^{\mathrm{T}}(k)}{\lambda + \left\|\boldsymbol{\phi}_2(k)\right\|^2}]\boldsymbol{E}(k)\\
&\quad + [\frac{\rho_2\boldsymbol{\phi}_2(k)\boldsymbol{\phi}_2^{\mathrm{T}}(k)}{\lambda + \left\|\boldsymbol{\phi}_2(k)\right\|^2} - I]\boldsymbol{\phi}_1(k)\Delta\boldsymbol{y}(k)
\end{aligned} \tag{55}$$

Because $\rho_1, \rho_2 \in (0, 1]$, $0 < \left\|\boldsymbol{\phi}_1(k)\right\| \leq b_1$, $0 < \left\|\boldsymbol{\phi}_2(k)\right\| \leq b_2$, $\lambda > 0$, $d_1 + d_2 \geq 2\sqrt{d_1 d_2}$, there must be an $0 < \psi < 1$ and $b_2 > 2\sqrt{\lambda}$ is selected at the same time, so that the following formula holds.

$$\begin{aligned}
0 < \psi < \left\| \frac{\boldsymbol{\phi}_2(k)\boldsymbol{\phi}_2^{\mathrm{T}}(k)}{\lambda + \left\|\boldsymbol{\phi}_2(k)\right\|^2} \right\| &= \frac{1}{\frac{\lambda}{\left\|\boldsymbol{\phi}_2(k)\right\|^2} + 1}\\
\leq \frac{\left\|\boldsymbol{\phi}_2(k)\right\|}{2\sqrt{\lambda}} \leq \frac{b_2}{2\sqrt{\lambda}} &< 1
\end{aligned} \tag{56}$$

So, (55) can be rewritten as

$$\begin{aligned}
\|\boldsymbol{E}(k+1)\| &= \left\| [\boldsymbol{I} - \frac{\rho_1 \times \boldsymbol{\phi}_2(k) \times \boldsymbol{\phi}_2^{\mathrm{T}}(k)}{\lambda + \left\|\boldsymbol{\phi}_2(k)\right\|^2}]\boldsymbol{E}(k) \right.\\
&\quad \left. + [\frac{\rho_2\boldsymbol{\phi}_2(k)\boldsymbol{\phi}_2^{\mathrm{T}}(k)}{\lambda + \left\|\boldsymbol{\phi}_2(k)\right\|^2} - \boldsymbol{I}]\boldsymbol{\phi}_1(k)\Delta\boldsymbol{y}(k) \right\|\\
&\leq \|(1-\rho_1\psi)\boldsymbol{E}(k)\| + \left\| (\frac{\rho_2 b_2}{2\sqrt{\lambda}} - 1)\boldsymbol{\phi}_1(k)\Delta\boldsymbol{y}(k) \right\|
\end{aligned} \tag{57}$$

The following formula can be obtained by recursion.

$$\begin{aligned}
&\|\boldsymbol{E}(k+1)\|\\
&\leq (1-\rho_1\psi)\|\boldsymbol{E}(k)\| + (\frac{\rho_2 b_2}{2\sqrt{\lambda}} - 1)b_1\varepsilon_1\\
&\leq (1-\rho_1\psi)^2\|\boldsymbol{E}(k-1)\| + (1-\rho_1\psi)(\frac{\rho_2 b_2}{2\sqrt{\lambda}} - 1)b_1\varepsilon_1\\
&\quad + (\frac{\rho_2 b_2}{2\sqrt{\lambda}} - 1)b_1\varepsilon_1\\
&\leq (1-\rho_1\psi)^k\|E(1)\| + \frac{(1-(1-\rho_1\psi)^k)}{\rho_1\psi}(\frac{\rho_2 b_2}{2\sqrt{\lambda}} - 1)b_1\varepsilon_1
\end{aligned} \tag{58}$$

in which $E(1) = \boldsymbol{y}_d(1) - \boldsymbol{y}(1)$, $\boldsymbol{y}_d(1) = \boldsymbol{y}_d(k)$ is the expected output, $\boldsymbol{y}(1) = \begin{bmatrix} 0 & 0 \end{bmatrix}^{\mathrm{T}}$ is the initial value and b_1, b_2, ρ_1, ρ_2, ε_1, λ, ψ are bounded, so $\boldsymbol{E}(k+1) = \boldsymbol{y}_d(k+1) - \boldsymbol{y}(k+1)$ is bounded and $\boldsymbol{y}(k)$ is also bounded. From the front, there are $\rho_1 = \rho_2 \in (0, 1]$ and $0 < \psi < 1$. In (56), there is $\frac{\rho_2 b_2}{2\sqrt{\lambda_{\min}}} - 1 = 0$ when $0 < \lambda_{\mathrm{mim}} \leq \lambda$, so $0 < 1 - \rho_1\psi \leq 1$, that is

$$\lim_{k\to\infty}(1-\rho_1\psi)^k = 0 \tag{59}$$

So

$$\begin{aligned}
&\lim_{k\to\infty}\|\boldsymbol{E}(k+1)\|\\
&\quad \leq \lim_{k\to\infty}(1-\rho_1\psi)^k\|\boldsymbol{E}(1)\|\\
&\qquad + \lim_{k\to\infty}\frac{(1-(1-\rho_1\psi)^k)}{\rho_1\psi}(\frac{\rho_2 b_2}{2\sqrt{\lambda_{\min}}} - 1)b_1\varepsilon_1\\
&\quad = 0
\end{aligned} \tag{60}$$

The size of the matrix is greater than zero, therefore $\lim_{k\to\infty}\|\boldsymbol{E}(k+1)\| = 0$.

As can be seen from the above, the system error will be bounded, and when k tends to infinity, the system error will also tend to zero.

Let $\|\boldsymbol{E}(k+1)\| \leq M_1$, according to the model-free adaptive control algorithm there is the following inequality.

$$\begin{aligned}
u(k) &\leq u(k-1) + \rho_1\boldsymbol{\phi}_2^{\mathrm{T}}(k) \times \frac{\boldsymbol{y}_d(k+1) - \boldsymbol{y}(k)}{\lambda + \left\|\boldsymbol{\phi}_2(k)\right\|^2}\\
&\quad + \rho_2\boldsymbol{\phi}_2^{\mathrm{T}}(k) \times \frac{\boldsymbol{\phi}_1(k)\Delta\boldsymbol{y}(k)}{\lambda + \left\|\boldsymbol{\phi}_2(k)\right\|^2}\\
&\leq u(k-1) + \frac{\rho_1 M_1}{2\sqrt{\lambda}} + \frac{\rho_2 b_1\varepsilon_1}{2\sqrt{\lambda}}
\end{aligned} \tag{61}$$

If the recursion idea is adopted for (61), there is

$$\begin{aligned}
u(k) &\leq u(k-1) + \frac{\rho_1 M_1}{2\sqrt{\lambda}} + \frac{\rho_2 b_1\varepsilon_1}{2\sqrt{\lambda}}\\
&\leq u(k-2) + 2\frac{\rho_1 M_1 + \rho_2 b_1\varepsilon_1}{2\sqrt{\lambda}}\\
&\leq u(1) + (k-1)\frac{\rho_1 M_1 + \rho_2 b_1\varepsilon_1}{2\sqrt{\lambda}}
\end{aligned} \tag{62}$$

In (62), ρ_1, ρ_2, b_1, ε_1, M_1, λ are bounded, therefore, $u(k)$ is also bounded.

According to the above analysis, it can be seen that the system is stable and the system error is convergent.

V. SIMULATION AND EXPERIMENT IMPLEMENTATION

In this section, some simulation and experiment results are presented to verify the practical control performance of the proposed method.

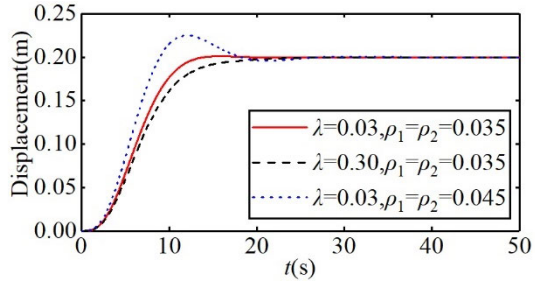

(a) Trolley displacement

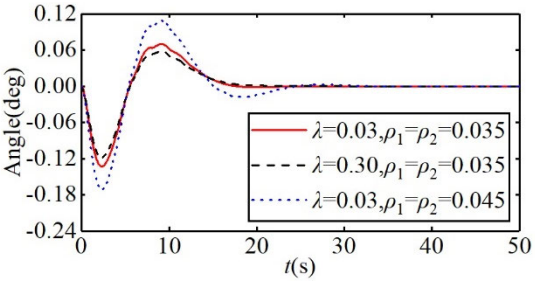

(b) Load swing angle

FIGURE 2. Simulation results of different parameters.

A. SIMULATION RESULTS AND ANALYSIS

In order to verify the effectiveness of the proposed MFAC control method, some simulations are conducted in the MATLAB/Simulink environment. Here, we choose the parameters of the system as

$$M = 6.50\ \text{kg}, \quad m = 2.00\ \text{kg}, \ l = 0.53\ \text{m}, \ p = 0.04$$

The desired position of the trolley is set as $x_d = 0.2$m. The initial parameters of model free adaptive control are set as

$$\mu = 1, \quad \eta = 1, \ \boldsymbol{\phi}_1(1) = \begin{bmatrix} 1.5 & 0.1 \\ 0.1 & 1.5 \end{bmatrix}, \ \boldsymbol{\phi}_2(1) = \begin{bmatrix} 1.5 \\ 0.1 \end{bmatrix},$$
$$u(1) = u(2) = 0, \quad \boldsymbol{y}(1) = \boldsymbol{y}(2) = \begin{bmatrix} 0 & 0 \end{bmatrix}^{\mathrm{T}}, \ \alpha_1 = 0.01,$$
$$\alpha_2 = 0.05.$$

Simulation Group 1: λ, ρ_1 and ρ_2 parameter selection

The values of λ, ρ_1 and ρ_2 will affect the control performance of the system. To select the appropriate parameter values, the following three cases are given.

$$\begin{aligned} &\text{Case 1: } \lambda = 0.03, \quad \rho_1 = \rho_2 = 0.035 \\ &\text{Case 2: } \lambda = 0.30, \quad \rho_1 = \rho_2 = 0.035 \\ &\text{Case 3: } \lambda = 0.03, \quad \rho_1 = \rho_2 = 0.045 \end{aligned}$$

The simulation results are shown in Fig. 2. Quantified results of three cases are shown in Table. 1.

The simulation results show when the penalty factor λ of the control force is changed separately, the larger λ is and the slower the trolley reaches the designated position, and the greater the load swing angle is. When the step factors ρ_1 and ρ_2 are changed, the greater the step factor ρ_1 and ρ_2 are, the faster the trolley reaches the specified position. However, the corresponding trolley displacement will produce overshoot, and the load swing angle is also be larger.

TABLE 1. Quantified results of three cases.

	t_s(s)	σ(%)	$\theta_{\max}$(deg)
Case1	13.86	0.42	0.14
Case2	17.22	0.31	0.12
Case3	24.86	15	0.17

Note: t_s and σ indicates the adjustment time and overshoot of the trolley displacement, $\theta_{\max}$ represents the maximum swing angle of the load.

According to Tab. 1, although the overshoot and load swing angle in Case 1 are slightly larger than those in Case 2, the adjustment time is 3.36 s shorter. After comprehensive consideration, $\lambda = 0.03$, $\rho_1 = \rho_2 = 0.035$ are selected and all performance indicators of the system are relatively good.

Simulation Group 2: Comparative study

The PID control method [26] is chosen for comparison. The incremental PID control law is given as

$$\begin{aligned} \Delta U_{pid} &= k_{xp}(e(k) - e(k-1)) + k_{xi}e(k) \\ &\quad + k_{xd}(e(k) - 2e(k-1) \\ &\quad + e(k-2)) + k_{\theta p}(e(k) - e(k-1)) + k_{\theta i}e(k) \\ &\quad + k_{\theta d}(e(k) - 2e(k-1) + e(k-2)) \end{aligned} \tag{63}$$

where $k_{xp} = 1$, $k_{xi} = 0.01$, $k_{xd} = 6$, $k_{\theta p} = -4$, $k_{\theta i} = 0.01$, $k_{\theta d} = -2$ are selected.

A pulse disturbance signal with a duration of 0.3 s and an amplitude of 4 N is added at 25 s. The simulation results are shown in Fig. 3.

It can be seen both methods can make the trolley reach the target position without residual swing angle of the load. But our method has faster trolley positioning speed and smaller load swing angle. When encountering matched disturbance, the MFAC method has smaller changes in trolley displacement and load swing angle, shorter recovery time and less control force than the PID method. The results indicate that the MFAC method has good tracking performance and strong anti-disturbance ability.

Simulation Group 3: Robustness study

To test the robustness of the control system, the rope length and load mass are changed while the MFAC controller parameters remain consistent. The three sets of data are selected as follows.

$$\begin{aligned} &\text{Case 1: } m = 2\ \text{kg}, \quad l = 0.53\ \text{m} \\ &\text{Case 2: } m = 3\ \text{kg}, \quad l = 0.53\ \text{m} \\ &\text{Case 3: } m = 2\ \text{kg}, \quad l = 0.43\ \text{m} \end{aligned}$$

The simulation results are shown in Fig. 4.

As can be seen from Fig.4, the proposed method can still achieve better positioning control and the maximum load swing angle is still relatively small while keeping the controller parameters unchanged. The results show that the system has strong robustness.

B. EXPERIMENTAL RESULTS AND ANALYSIS

In order to further validate the practical control performance of MFAC approach, we conduct some experiments on the

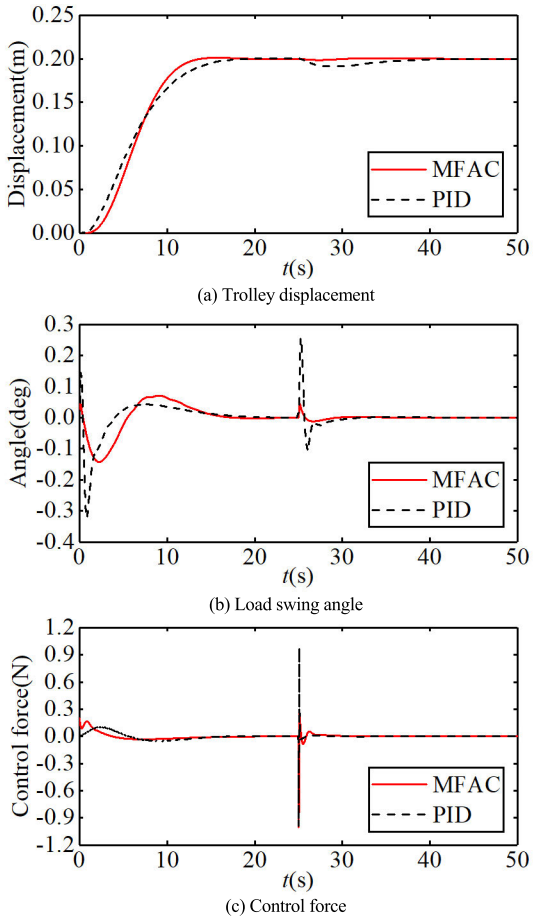

FIGURE 3. Simulation results for contrast method under disturbance.

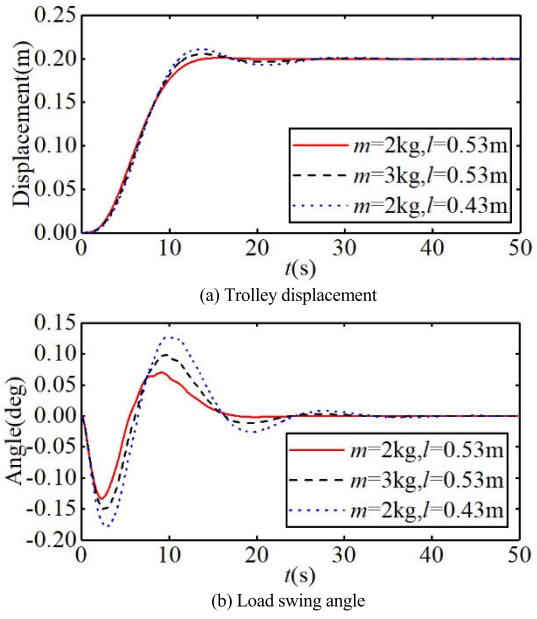

FIGURE 4. Simulation result of different model parameters.

bridge crane experimental platform. The experimental platform is shown in Fig. 5.

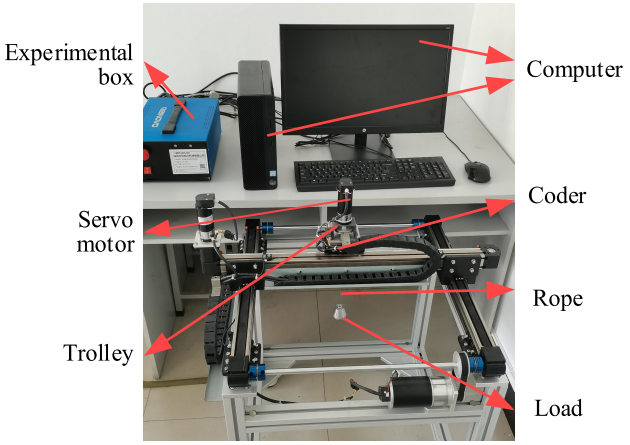

FIGURE 5. Bridge crane experimental platform.

In Fig.5, the trolley is driven by DC servo motor, the coders are used to measure trolley displacement and load swing angle. The experimental box includes a motion control module and a servo drive module. The motion control module reads information from the coders and sends it to the computer for generating real-time control commands, which are sent to the servo drivers to control the motors. The control algorithm runs in the environment MATLAB/Simulink, and the sampling period is set as 0.01 s. The MFAC algorithm (35) and the Pseudo-Jacobian matrix estimation algorithm (38) are written using the S function on MATLAB/Simulink.

In this experiment study, the physical parameters are configured as:

$$M = 1.55\ \text{kg}, \quad m = 0.22\ \text{kg}, \ l = 0.20\ \text{m}, \ p = 0.04.$$

The desired position of the trolley is x_d =0.10 m. The initial parameters of model free adaptive control are

$$\mu = 1, \quad \eta = 1, \ \boldsymbol{\phi}_1(1) = \begin{bmatrix} 0.2 & 0.5 \\ 0.1 & 0.3 \end{bmatrix}, \ \boldsymbol{\phi}_2(1) = \begin{bmatrix} 1.5 \\ 0.1 \end{bmatrix},$$
$$u(1) = u(2) = 0, \quad \boldsymbol{y}(1) = \boldsymbol{y}(2) = \begin{bmatrix} 0 & 0 \end{bmatrix}^{\mathrm{T}}, \ \alpha_1 = 0.01,$$
$$\alpha_1 = 0.05.$$

Experiment Group 1: λ, ρ_1 and ρ_2 parameter selection

In order to verify the influence of different MFAC parameters λ, ρ_1 and ρ_2 on the control performance, the following three cases are selected.

$$\text{Case 1: } \lambda = 0.03, \quad \rho_1 = \rho_2 = 0.042$$
$$\text{Case 2: } \lambda = 0.30, \ \rho_1 = \rho_2 = 0.042$$
$$\text{Case 3: } \lambda = 0.03, \ \rho_1 = \rho_2 = 0.060$$

The experimental results of trolley displacement and load swing angle are shown in Fig. 6.

Using the same principles as the simulation group 1, parameters $\lambda = 0.03$, $\rho_1 = \rho_2 = 0.042$ are selected according to Fig.6.

Experiment Group 2: Comparative study

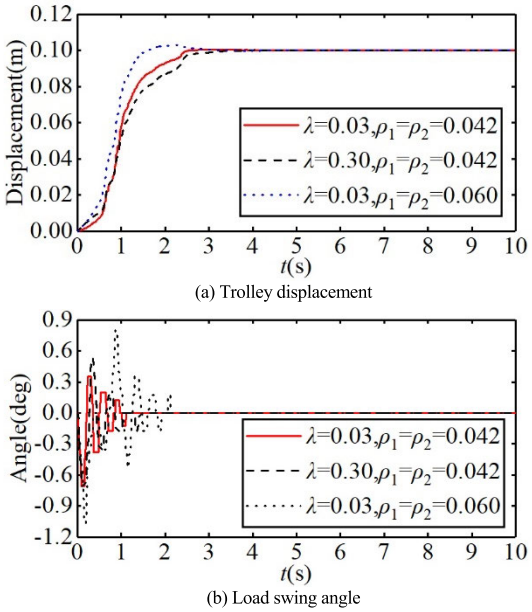

(a) Trolley displacement

(b) Load swing angle

FIGURE 6. Experimental results of different controller parameters.

In experimental study, the PID parameters of refence [26] are selected as following.

$$k_{xp} = 5, \quad k_{xi} = 0.01, \; k_{xd} = 6, \; k_{\theta p} = -2,$$
$$k_{\theta i} = 0.01, \quad k_{\theta d} = -1.$$

When the trolley runs to 4.9 s, a pulse disturbance signal with duration of 0.3 s and amplitude of 4 N is added to the system in the control channel.

The experimental results of two control methods are shown in Fig.7.

It can be seen from the experimental results from Fig.7 that the MFAC method is faster than the PID method in trolley positioning and anti-swing. When the disturbance is added, both the PID method and the proposed method can make the trolley displacement return to the designated position after a period of time. The load swing angle can also reach a stable state. However, compared with the PID control method, this proposed method has shorter trolley positioning time, smaller load swing amplitude and less control force which verifies that the positioning and anti-swing control effect of the proposed controller is better than the PID control method.

Experiment Group 3: Robustness study

To test the robustness of MFAC, the rope length and load mass are changed while the MFAC controller parameters keep unchanged. The two sets of data are selected as follows.

$$\text{Case 1: } m = 0.22 \text{ kg}, \quad l = 0.40 \text{ m}$$
$$\text{Case 2: } m = 0.42 \text{ kg}, \quad l = 0.20 \text{ m}$$

The corresponding experimental results are shown in Fig. 8.

It can be seen from the experimental results in Fig. 8 that when the mass and rope length change, the trolley displacement and load swing angle will change, but the changes are within a certain allowable range. The experimental results indicate that the proposed method has satisfactory robustness with respect to parameter changes.

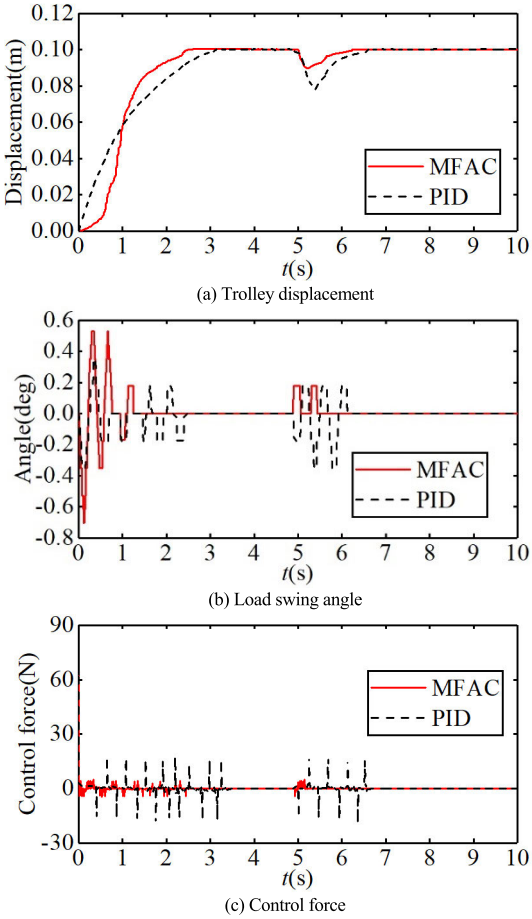

(a) Trolley displacement

(b) Load swing angle

(c) Control force

FIGURE 7. Experimental results of different methods under disturbance.

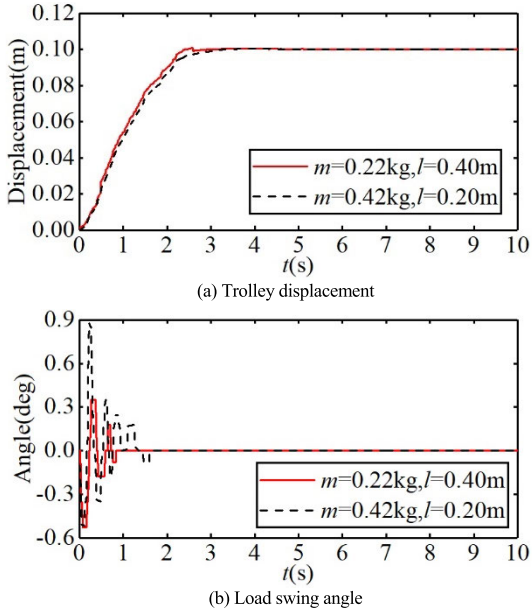

(a) Trolley displacement

(b) Load swing angle

FIGURE 8. Experiment of different system parameters.

VI. CONCLUSION

In this paper, we have proposed a data-driven model-free adaptive positioning and anti-swing control for bridge cranes. The full-format dynamic linearized data model of the bridge crane system is obtained by input and output data and a model-free adaptive control strategy is designed on the basis of data-driven model. The stability of the closed-loop system is proved through strict theoretical analysis. The effectiveness of this method is verified on the simulation and experiment platform. The proposed control method has a simple structure, good tracking performance and strong robustness for bridge cranes. However, designing the controller requires a large amount of system input and output data, which puts forward higher requirements for the accuracy and rapidity of testing equipment.

In practice, the bridge crane system is generally considered as a 3D system, which has a more complex model structure than 2D. At present, we have conducted some theoretical research on the application of this method in 3D bridge crane system, and the positioning and anti-swing control results will be given in the subsequent research work.

REFERENCES

[1] M. Zhang, X. Ma, R. Song, X. Rong, G. Tian, X. Tian, and Y. Li, "Adaptive proportional-derivative sliding mode control law with improved transient performance for underactuated overhead crane systems," *IEEE/CAA J. Autom. Sinica*, vol. 5, no. 3, pp. 683–690, May 2018.

[2] D. Chwa, "Sliding-mode-control-based robust finite-time antisway tracking control of 3-D overhead cranes," *IEEE Trans. Ind. Electron.*, vol. 64, no. 8, pp. 6775–6784, Aug. 2017.

[3] T. Wang, N. Tan, X. Zhang, G. Li, S. Su, J. Zhou, J. Qiu, Z. Wu, Y. Zhai, D. L. Ruggero, V. Piurit, and F. Scotti, "A time-varying sliding mode control method for distributed-mass double pendulum bridge crane with variable parameters," *IEEE Access*, vol. 9, pp. 75981–75992, 2021.

[4] W. Yang, J. Chen, D. Xu, and X. Yan, "Hierarchical global fast terminal sliding-mode control for a bridge travelling crane system," *IET Control Theory Appl.*, vol. 15, no. 6, pp. 814–828, Apr. 2021.

[5] G. O. Tysse, A. Cibicik, L. Tingelstad, and O. Egeland, "Lyapunov-based damping controller with nonlinear MPC control of payload position for a knuckle boom crane," *Automatica*, vol. 140, pp. 1–12, Jan. 2022.

[6] J. Smoczek and J. Szpytko, "Particle swarm optimization-based multivariable generalized predictive control for an overhead crane," *IEEE/ASME Trans. Mechatronics*, vol. 22, no. 1, pp. 258–268, Jun. 2017.

[7] R.-C. Roman, R.-E. Precup, and E. M. Petriu, "Hybrid data-driven fuzzy active disturbance rejection control for tower crane systems," *Eur. J. Control*, vol. 58, pp. 373–387, Mar. 2021.

[8] Z. Sun, J. Zhou, Y. Ling, X. Xie, Y. Yu, and Z. Sun, "Designing and application of modified SSA based ADRC controller for overhead crane systems," *Int. J. Intell. Robot. Appl.*, vol. 6, no. 3, pp. 449–466, Jan. 2022.

[9] L. V. Duong and L. A. Tuan, "Modeling and observer-based robust controllers for telescopic truck cranes," *Mechanism Mach. Theory*, vol. 173, pp. 94–114, Jul. 2022.

[10] G. Rigatos, P. Siano, and M. Abbaszadeh, "Nonlinear H-infinity control for 4-DOF underactuated overhead cranes," *Trans. Inst. Meas. Control*, vol. 40, no. 7, pp. 2364–2377, Apr. 2018.

[11] Z. S. Hou and X. H. Bu, "Model free adaptive control with data dropouts," *Expert Syst. Appl.*, vol. 38, no. 8, pp. 10709–10717, Aug. 2011.

[12] C. De Persis and P. Tesi, "Formulas for data-driven control: Stabilization, optimality, and robustness," *IEEE Trans. Autom. Control*, vol. 65, no. 3, pp. 909–924, Mar. 2020.

[13] F. Memon and C. Shao, "Data-driven optimal PID type ILC for a class of nonlinear batch process," *Int. J. Syst. Sci.*, vol. 52, no. 2, pp. 263–276, Jan. 2021.

[14] T. Kinoshita, Y. Morota, and T. Yamamoto, "Design of a data-driven multi PID controllers using ensemble learning and VRFT," *J. Robot., Netw. Artif. Life*, vol. 7, no. 1, pp. 68–72, May 2020.

[15] R. Chi, H. Li, D. Shen, Z. Hou, and B. Huang, "Enhanced P-type control: Indirect adaptive learning from set-point updates," *IEEE Trans. Autom. Control*, vol. 68, no. 3, pp. 1600–1613, Mar. 2023.

[16] H. Liang, R. Chi, Y. Lv, Y. Sun, and D. Kong, "Data-driven stochastic optimal iterative learning control for nonlinear non-affine systems with measurement data loss," *IEEE Access*, vol. 7, pp. 133069–133078, 2019.

[17] M. R. Estakhrouiyeh, A. Gharaveisi, and M. Vali, "Fractional order proportional-integral-derivative controller parameter selection based on iterative feedback tuning. Case study: Ball levitation system," *Trans. Inst. Meas. Control*, vol. 40, no. 6, pp. 1776–1787, Apr. 2018.

[18] R.-C. Roman, R.-E. Precup, E.-L. Hedrea, S. Preitl, I. A. Zamfirache, C.-A. Bojan-Dragos, and E. Petriu, "Iterative feedback tuning algorithm for tower crane systems," *Proc. Comput. Sci.*, vol. 199, pp. 157–165, Jan. 2022.

[19] Y. Yuan and L. Tang, "Novel time-space network flow formulation and approximate dynamic programming approach for the crane scheduling in a coil warehouse," *Eur. J. Oper. Res.*, vol. 262, no. 2, pp. 424–437, 2017.

[20] H. N. Esfahani and R. Szlapczynski, "Robust-adaptive dynamic programming-based time-delay control of autonomous ships under stochastic disturbances using an actor-critic learning algorithm," *J. Mar. Sci. Technol.*, vol. 26, no. 4, pp. 1262–1279, Dec. 2021.

[21] Z. Hou, C. Han, and W. Huang, "The model-free learning adaptive control of a class of miso nonlinear discrete-time systems," *IFAC Proc. Volumes*, vol. 31, no. 25, pp. 227–232, Sep. 1998.

[22] S. Xiong and Z. Hou, "Model-free adaptive control for unknown MIMO nonaffine nonlinear discrete-time systems with experimental validation," *IEEE Trans. Neural Netw. Learn. Syst.*, vol. 33, no. 4, pp. 1727–1739, Apr. 2022.

[23] R.-C. Roman, R.-E. Precup, E. M. Petriu, E.-L. Hedrea, C.-A. Bojan-Dragos, and M.-B. Radac, "Model-free adaptive control with fuzzy component for tower crane systems," in *Proc. IEEE Int. Conf. Syst., Man Cybern. (SMC)*, Bari, Italy, Oct. 2019, pp. 1384–1389.

[24] X. Gu, B. Xian, and J. Li, "Model free adaptive control design for a tilt trirotor unmanned aerial vehicle with quaternion feedback: Theory and implementation," *Int. J. Adapt. Control Signal Process.*, vol. 36, no. 1, pp. 122–137, Jan. 2022.

[25] S. A. Hashjin, S. Pang, E.-H. Miliani, K. Ait-Abderrahim, and B. Nahid-Mobarakeh, "Data-driven model-free adaptive current control of a wound rotor synchronous machine drive system," *IEEE Trans. Transport. Electrific.*, vol. 6, no. 3, pp. 1146–1156, Sep. 2020.

[26] Z. Sun, Y. Ling, X. Tan, Y. Zhou, and Z. Sun, "Designing and application of type-2 fuzzy PID control for overhead crane systems," *Int. J. Intell. Robot. Appl.*, vol. 5, no. 1, pp. 10–22, Mar. 2021.

XUEJUAN SHAO received the M.S. and Ph.D. degrees in control science and engineering from the Taiyuan University of Science and Technology, Taiyuan, China, in 2005 and 2021, respectively. She is an Associate Professor with the School of Electronics and Information Engineering, Taiyuan University of Science and Technology. Her research interests include the control of underactuated crane systems and the control of electric drives.

XIUJIAN ZOU received the B.S. degree in electrical engineering and automation from Jiamusi University, Jiamusi, China, in 2020. He is currently pursuing the M.S. degree in control science and engineering with the Taiyuan University of Science and Technology, Taiyuan, China. His current research interests include data-driven control and bridge crane systems.

JINGGANG ZHANG received the M.S. and Ph.D. degrees in control science and engineering from the Harbin Institute of Technology, Harbin, China, in 1989 and 2008, respectively. He is currently a Professor with the School of Electronics and Information Engineering, Taiyuan University of Science and Technology, China. His research interests include data-driven control and robust control for nonlinear systems.

ZHICHENG ZHAO received the B.S. degree in automation from the Taiyuan University of Technology, Taiyuan, China, in 1992, and the M.S. degree in automation from the Taiyuan Heavy Machinery Institute, Taiyuan, in 1999. He is currently a Professor with the School of Electronics and Information Engineering, Taiyuan University of Science and Technology. His research interests include advanced control, computer measurement and control systems, and devices.

ZHIMEI CHEN received the M.S. degree in automation from Taiyuan Heavy Machinery Institute, Taiyuan, China, in 1998, and the Ph.D. degree in control science and engineering from the Taiyuan University of Science and Technology, Taiyuan, in 2011. She is currently a Professor with the School of Electronics and Information Engineering, Taiyuan University of Science and Technology. Her research interests include robust control and intelligent control of the electromechanical integration systems.

LIANGLIANG ZHOU received the B.S. degree in automation from the Beijing University of Science and Technology, Beijing, China, in 2006. Currently, he is the Deputy Director of the Electrical Institute of Taizhong Company Ltd. His research interests include ac motor drive, electric drive and its automation, industrial control and intelligent research, and the development of related equipment.

ZHENYAN WANG received the M.S. degree in automation from the University of Science and Technology, Taiyuan, China, in 1998, and the Ph.D. degree in control science and engineering from the Beijing University of Aeronautics and Astronautics, Beijing, China, in 2014. She is currently an Associate Professor with the School of Electronics and Information Engineering, Taiyuan University of Science and Technology. Her research interests include nonlinear system control and sliding mode control.